A Linear Feature Mapping Framework for Adaptive Detection and Recognition of Targets in Complex SAR Data *

X. Yu*+, L. E. Hoff**, I. S. Reed+, A. M. Chen*, D. Buck**

SAIC* San Diego, CA 92121

NCCOSC** San Diego, CA 92152

USC+ Los Angeles, CA 90089

Abstract

In this paper a framework for automatic target detection/recognition (ATD/R) system that incorporates modern image processing into classical hypothesis detection theory is presented. The technique is based upon the linear feature map detector derived in [1]. The algorithm is extended here to target recognition and applied to the complex SAR data collected by the SRI UHF Ultra-wideband radar which is supported in part by MIT/Lincoln Laboratory. A linear feature mapping such as the Discrete Cosine Transform (DCT) or the Wavelet Transform (WT) are used to achieve an effective feature representation for target detection and recognition. The effectiveness of the representation is evaluated not only by the number of features, i.e. the dimension of the subspace, needed to represent a target signal for a given mean-square error, but also by the separability of such target features from clutter background and other target classes.

1 Introduction

Recently a new matched-filter based adaptive detector which uses linear feature mappings is developed for the complex data domain of SAR [1]. This linear-feature mapping detector enhances the signal-to-clutter ratios available for detection by exploiting the differences between the subspaces in which significant target and clutter energy lie. The performance of this detector is completely analyzed and shown to have the property of a Constant False Alarm Rate (CFAR). Preliminary results of target feature modeling for detection are tested by the use of actual SRI SAR data [2]. The detection experiments demonstrate that a receiver-operating-characteristic (ROC) curve performance improvement of 1.5 orders of magnitude at $P_d = 80\%$ over an amplitude-only 2-parameter CFAR detector, where P_d denotes the probability of detection.

The success of an ATR system depends not only on its ability to detect objects from clutter but also to discriminate *targets* from all other possible target-like objects. Most ATR systems have a target classifier following the designed detector to further reduce the number of false alarms, which are caused by trees, clutter discretes and nontarget objects that are detected incorrectly. The wide variety of possible target classes make it almost impossible to know *a priori* the distribution of the available target classes. Therefore, a standard Bayesian classifier is not suitable to this application. Typical solutions for the problem involve measuring the distance of the object from the target mean and then applying a threshold or a ranking to determine whether or not an object is a target [3], [4]. For these techniques the classifications are often performed on the original observation data. However, in practice the targets are located behind and under tree foliage and therefore the observations are strongly influenced by the background clutter. The distance measures obtained from the clutter-contaminated observations definitely misleads the decision of a classifier. Moreover, the dimensionality of the observation space is often higher than that of the intrinsic dimensionality of the target or the number of significant features required for classification.

In this paper a linear feature-mapping classification (LFMC) criterion is proposed as a natural follow-up to a linear feature-mapping detection criterion. By properly selecting a transform or feature domain, the clutter interference can often be considerably suppressed since target energy and clutter energy are usually better separated in the transform domain. For example, if the target and clutter lie in a different spatial frequency band (or have a different spatial resolution),

*This work was funded by ARPA War Breaker Program under Contract N66001-91-D-0046.

1058-6393/95 $4.00 © 1995 IEEE

the corresponding coefficients of a Fourier transform (or a wavelet transform) that significantly characterize the target usually interfer less than in the original observation domain. There are various linear feature mappings and representations. It is well-known that the Karhunen-Loeve expansion is optimum for the purpose of random signal representation [5]. However, the target covariance matrix is usually unknown and is difficult to measure, using observations within a scene. Hence, the KL expansion is rarely used in practice as a target representation. In this paper DCT suboptimal basis vectors are studied to achieve the newly developed LFMC criterion.

2 Linear Feature Mappings and Representations for Classification

First let

$$\underline{x} = [x_1, x_2, \ldots, x_N]^T \quad (1)$$

denote the N-vector formed by row ordering the pixels of the complex subimage of the observation data. Next let $\underline{s}$ be the complex pattern vector of target reflectivity, also formed in a row ordering, to be detected. Finally, assume that the data vector $\underline{x}$ equals approximately the signal $\underline{s}$ plus a clutter-plus-noise vector $\underline{n}$, i.e.,

$$\underline{x} = \underline{s} + \underline{n} \quad (2)$$

where $\underline{s} \in \mathbf{S}$ is an N-dimensional complex target vector, and $\mathbf{S}$ consists of *all* possible patterns obtained by imaging the target from a fixed viewing angle.

It is well-known that by choosing a proper set of basis vectors, one can always represent the signal by the expansion,

$$\underline{s} = \sum_{n=1}^{K} \underline{\phi}_n b_n + \underline{e} = \Phi_K \underline{b}_K + \underline{e} \quad (3)$$

with

$$\Phi_K = [\underline{\phi}_1, \underline{\phi}_2, \ldots, \underline{\phi}_K] \ , \ \underline{b}_K = [\underline{b}_1, \underline{b}_2, \ldots, \underline{b}_K] \ , \quad (4)$$

where the column vectors of Φ_K, i.e. ϕ_k for $k = 1, 2, \ldots, K$, are called the **significant features**. The vector $\underline{b}_K$ is the feature component vector and an element of $\underline{b}_K$, namely b_k, is called the value of the k-th feature in the **feature space**. Evidently $\underline{e}$ is the error vector due to the approximation of K features where $K \leq N$.

There are various linear feature mappings and representations. If a signal is random, it is well-known that the optimum choice for the feature vector is the eigenvector of the covariance matrix of the signal, i.e. the Karhunen-Loeve expansion. Since the signal covariance matrix is usually unknown and difficult to measure by using local observations, the KL expansion is rarely used in practice. Other possible suboptimal basis vectors include those from conventional image transforms, discrete Fourier transform (DFT) and discrete cosine transform (DCT), to the modern multiresolution decompositions, i.e. the wavelet transform (WT).

To measure the effectiveness of a subset of K features or basis vectors, one can use the mean-square magnitude of $\underline{e}(K)$ as a part of the criterion. The significant features, i.e. the features which carry most of the signal energy, are extracted with a selection mask in the transform domain. Note that the effectiveness of these significant features is evaluated not only by the number of features needed to represent a target signal for a given square magnitude error of approximation, but also by the separability of those features from the clutter background and other target classes. To demonstrate that the significant features of a HEMTT are effectively different from those of clutter, a comparison is made in terms of the percentage of the least-squares approximation error that resulted from using the HEMTT significant feature vectors to represent the clutter subregions as well as the HEMTT. In Fig. 1, the curves show that the approximation error of the clutter patches are large compared with those of the HEMTT. Hence, the optimum number of effective features K is that number which allows the largest separability between clutter and a target. At the same time, those effective features also allow for a large separability between the HEMTT and other types of vehicles, as shown in Fig. 2.

3 One-class classfier with a linear feature mapping

The incorporation of the feature mappings discussed in sec. 2 into a certain classification criteria leads to the following one-class classifier. This new classifier allows for further discrimination of a *desired object class* from clutter and all other possible objects by exploiting the incomplete prior knowledge of the statistical properties of both the clutter and the other target-like objects. For this one-class classification problem, the desired object class is called the *target class* and all other possible objects and false alarms caused by clutter discretes are called *nontargets*. In this paper, the *target class* consists of all possible patterns obtained by imaging a specific object from a fixed viewing angle with a SAR system. The set of target patterns is denoted by $\underline{s} \in \mathbf{S}$

The classifier uses the MLE of the feature components of a target signal in the feature space, which is defined in Sec. 2 as the vector $\underline{b}_K$, in order to discriminate the detections. The feature component vector $\underline{b}_K$ is different for each element $\underline{s}$ in $\mathbf{S}$. In order to compute the MLE of the unknown weights b_k of target signal $\underline{s}$ in (3) from a clutter-contaminated observation vector $\underline{x}$, first consider the probability density function of $\underline{x}$ under H_1, namely,

$$L(\underline{b}, \underline{x}|H_1) = \frac{1}{(\pi)^N |M|} e^{-(\underline{x}-\Phi_K \underline{b}_K)^h M^{-1} (\underline{x}-\Phi_K \underline{b}_K)}, \tag{5}$$

where $M = \mathbf{E}\{[\underline{x}-\mathbf{E}\underline{x}][\underline{x}-\mathbf{E}\underline{x}]^h\} = (N \times N)$ covariance matrix of clutter background. The vector $\tilde{\underline{b}}_K$ which achieves the maximum of $L(\underline{b}, \underline{x})$ for every data vector $\underline{x}$ is shown easily to be

$$\tilde{\underline{b}}_K = (\Phi_K^h M^{-1} \Phi_K)^{-1} \Phi_K^h M^{-1} \underline{x}\,. \tag{6}$$

Generally, in most practical problems the covariance M is not known, so that an estimate, such as the MLE of $\hat{M}$, defined by

$$\hat{M} = \frac{1}{L} \sum_{l=1}^{L} \underline{y}_l \underline{y}_l^h = \frac{1}{L} Y Y^h \tag{7}$$

is used as a replacement for M. If this substitution is made for an observation data vector $\underline{x}$, which has been tested to possibly contain the target, the maximum likelihood estimate (MLE) of $\underline{b}_K$ is given by

$$\hat{\underline{b}}_K = (\Phi_K^h \hat{M}^{-1} \Phi_K)^{-1} (\Phi_K^h \hat{M}^{-1} \underline{x}) \tag{8}$$

Then the one-class classifier, using feature component vector is given by

$$\rho = \frac{|\underline{b}_K^h \hat{\underline{b}}_K|^2}{||\underline{b}_K||^2\, ||\hat{\underline{b}}_K||^2} \begin{array}{ll} \geq & \rho_0 \text{ then } H_1 \\ < & \rho_0 \text{ then } H_0 \end{array}, \quad 0 \leq \rho \leq 1 \tag{9}$$

where ρ is related to the sample-correlation coefficient of the estimated feature component vector $\hat{\underline{b}}_K$ and $\underline{b}_K$. Here $\hat{\underline{b}}_K$ is obtained by using the observation data as shown in Eq. (8), and $\underline{b}_K$ is obtained by using apriori signature data. The probability density function of ρ is proved to be a Beta-distribution.

The relation of the MLE of the feature component vector $\underline{b}_K$ given in Eq. (9) for classification with the LMFD statistics r in [1] can be find by rewrite r as follows,

$$\begin{aligned} r &= \underline{x}^h \hat{M}^{-1} \Phi_K (\Phi_K^h \hat{M}^{-1} \Phi_K)^{-1} \Phi_K^h \hat{M}^{-1} \underline{x} \\ &= \underline{x}^h \hat{M}^{-1} \Phi_K \hat{\underline{b}}_K\,. \end{aligned} \tag{10}$$

Eq. (10) indicates the fact that if K is the number of features used for detection and I is the number of extra features required to be added for finer classification, then the computation of the estimated feature component vector $\hat{\underline{b}}_{K+I}$ can be based on the already computed vector $\hat{\underline{b}}_K$ in LFMD process with about the same order needed to invert an $I \times I$ matrix.

4 Experimental Results of Classification Using Feature Mapping

To evaluate the performance of the ATR system using the linear feature mapping, experiments on actual SAR data were performed. The data were collected by the SRI FOPEN II Ultra Wide Band, HH-polarization, 1 meter resolution SAR. In particular, two scenes from the Portage, Maine, area were used for the study: The Signature Array Site and the Illustative-Example Site. The Signature Array image consisted of a number of trucks (targets) in an open grassy field that were also used to determine the target features at a particular radar viewing angle.

The Illustrative-Example image in Fig. 3 consists of twelve military vehicles (three are camouflaged), i.e. HEMTTs, 2.5-ton trucks, and 5-ton trucks, located behind and under tree foliage. The vehicles in the site are positioned so that they are approximately at broadside with respect to the radar look angle. *HEMTT1* through *HEMTT4* denote HEMTTs, *NT1* through *NT9* are either 2.5-ton trucks or 5-ton trucks, *CAMO* is the deployed empty camouflage net, and *CRA* thru *CRD* denote the four-corner reflectors in the site.

Since the goal of this paper is to detect and recognize HEMTTs, the HEMTT is called the target and the other types of vehicles are called non-targets. After applying the linear feature mapping detector to match the subspace, spanned by $K = 16$ feature vectors which carry significant information of HEMTT at broadside, the detection results are shown in Fig. 4. Here the threshold is set to obtain 100% detection of the HEMTTs in the scene. As indicated in Fig. 4, three false alarms are detected simultaneously with the four HEMTTS: One is due to clutter and the other two are due to the non-target vehicles. The corresponding maximum-statistic values of these seven "targets" declared by the LFMD are shown in Fig. 5a.

To further discriminate the HEMTTs against other non-targets, the detected potential targets are fed into the LFMC. Because a single target can produce multiple CFAR detections, the detected pixels are clustered if they are within the target-sized neighborhood. Then an 8×16 pixel window is used to extract the region of interest from the original image and passed to the classifier for further processing. Figs. 5b and 5c give the output classification test statistics for the seven detected potential targets using DCT feature maps for $K = 16$ while $I = 16$ and $I = 48$, respectively. The statistics indicate that there is substantial performance gain in adding further features and processing beyond the detection stage. The classifier has effectively reduced the number of false alarms to zero.

5 Conclusion

A one-class classifier, which uses a MLE of the feature component vector, enhances significantly the differences between actual targets and nontargets. Therefore, the classification after detection further reduces the false-alarm rate substantially. For example, by applying the LFMC to recognize HEMTTs at broadside angle, which are contained in a set of actual SAR data after using the LMFD criterion, the number of false alarms is reduced from $25/Km^2$ to zero. Thus the ATD/R which uses a linear feature-mapping framework is quite powerful and promising for future SAR image data processing applications.

References

[1] X. Yu and I. S. Reed, *"Adaptive Detection of Signals with Feature Linear Mappings and Representations,"* submitted to IEEE Trans. on Signal Processing.

[2] X. Yu, L.E. Hoff, I. S. Reed, D. Buck, and A. M. Chen, *"Comparative Study of Feature Mapping and Selection for ATR: Experiments on SAR Data,"* SPIE Conference Proceedings- Optical Engineering in Aerospace Sensing, Orlando, Florida, April 1994.

[3] L. M. Novak, *Optimal Target Designation Techniques*, IEEE Trans. on Aerospace and Electronic Systems, vol AES-17, No. 5, Sept. 1981.

[4] K. Fukunaga, R. R. Hayes and L. M. Novak, *The Acquisition Probability for a Minimum Distance One-Class Classifier*, IEEE Trans. on Aerospace and Electronic Systems, vol. AES-23, No. 4, July 1987.

[5] Y. T. Chien and K. S. Fu, *"Selection and Ordering of Feature Observations in a Pattern Recognition System*, Information and Control, 12, pp. 395-414, 1968.

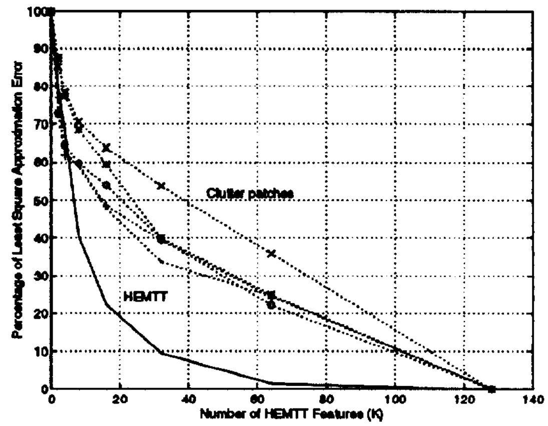

Figure 1: Comparisons of the percentage of least-squares approximation error using the significant features of HEMTT in the DCT domain to represent HEMTT and several clutter patches. Large least squares approximation errors for clutter patches indicate that the effective features for HEMTT are significantly different from those of the clutter patches.

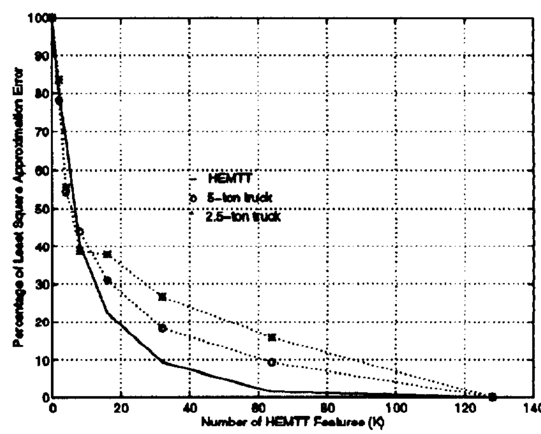

Figure 2: Comparison of percentages of least-squares approximation error using the significant features of the HEMTT in the DCT domain to represent HEMTT and other non-targets.

Figure 3: Illustrative-Example SAR image of the SRI FOPEN II ultra-wideband SAR system with HH-polarization, and a 1 meter resolution.

Figure 4: Automatic target detection results by applying the linear-feature map detector to the Illustrative-Example Site of Fig. 4. The results yield 100% detection of HEMTTs in the scene using DCT linear feature map with the number of significant features being $K = 16$ out of 128.

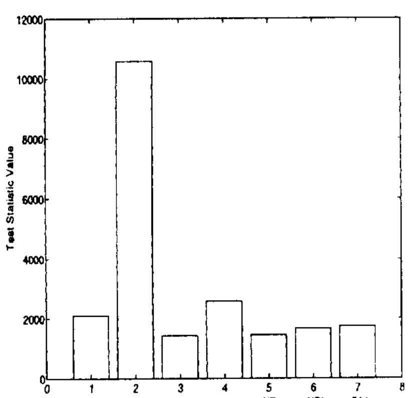

(a) Local maximum-statistic values around the locations of the detected 4 HEMTTs and 3 nontargets for K=16.

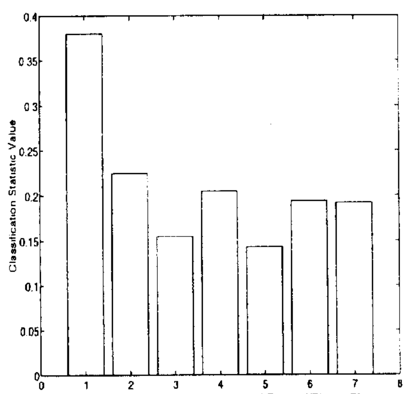

(b) The classification-statistic values at the locations of the detected 4 HEMTTs and 3 nontargets for K=32.

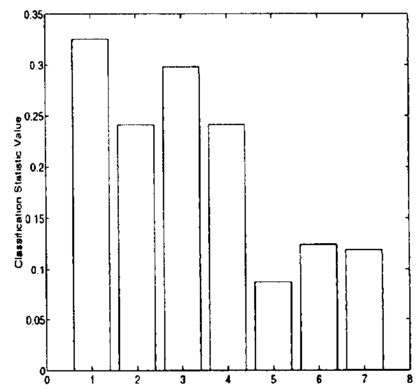

(c) The classification-statistic values at the locations of the detected 4 HEMTTs and 3 nontargets for K=64.